Steric Interactions in a Model Multimembrane System: A Synchrotron X-Ray Study

C. R. Safinya,[1] D. Roux,[1,3] G. S. Smith,[1,2] S. K. Sinha,[1] P. Dimon,[1] N. A. Clark,[2] and A. M. Bellocq[3]

[1]*Exxon Research and Engineering Company, Annandale, New Jersey 08801*
[2]*Department of Physics, University of Colorado, Boulder, Colorado 80309*
[3]*Centre de Recherche Paul Pascal and Groupement de Recherches Coordinées de Microemulsion, Centre National de la Recherche Scientifique, 33405 Talence, Bordeaux, France*

(Received 12 August 1986)

We report a high-resolution x-ray study of a model multilayer fluid membrane system in the lyotropic L_α phase of a quaternary microemulsion system. The structure factor exhibits power-law behavior characteristic of a Landau-Peierls system. As a function of intermembrane distance 3.8 nm $\leq d \leq$ 16.3 nm, the exponent $\eta(d)$ which describes the algebraic decay of layer correlations is predicted by the model of Helfrich where entropic steric repulsions dominate intermembrane interactions.

PACS numbers: 61.30.Eb, 82.70.Kj

The physical properties of multilayer membrane systems, which consist of equally spaced fluid bilayer lipid sheets embedded in water, have long been subjects of intense interest in biophysical research. In particular, much attention has been focused on the understanding of intermembrane interactions. The basic forces[1] between two parallel membrane sheets involve long-range van der Waals interactions, and short-range repulsive hydration and screened electrostatic forces. Recently, Helfrich[2] has proposed that large, thermally induced, out-of-plane layer fluctuations give rise to a repulsive interaction between membranes because of steric hindrance in multilayer systems. More generally, steric repulsions are known to be the dominant interactions associated with wandering walls of incommensurate phases.[3] This interaction has been calculated[2] for a multilayer system by use of the Landau–de Gennes[4,5] elastic theory of smectic-A liquid crystals with energy density

$$F/V = \{B(\partial u/\partial z)^2 + K[(\partial^2 u/\partial x^2) + (\partial^2 u/\partial y^2)]^2\}/2 , \quad (1)$$

where $u(\mathbf{r})$ is the layer displacement in the z direction normal to the layers, and B and K are the bulk moduli for layer compression (erg/cm^3) and layer curvature (erg/ cm). The free energy of steric interaction per unit area for two membranes separated by a distance d is[2] $U_s/A = \alpha k_B T/d^2$, where $\alpha = 0.23 k_B T/k_c$ and k_c is the elastic modulus for curvature for a single membrane ($K = k_c N$, where N is the number of layers per unit height). The van der Waals interaction is given by[1]

$$\frac{U_{\rm vdW}}{A} \sim -\frac{H}{12\pi}\left[\frac{1}{d^2} - \frac{2}{(d+\delta)^2} + \frac{1}{(d+2\delta)^2}\right] ,$$

which for $d \gg \delta$ gives $\sim -H\delta^2/d^4$, where δ is the membrane thickness and $H \sim 0.75 k_B T$ is the Hamaker constant. Thus, the Helfrich interaction competes in range with the van der Waals attraction and should dominate at large intermembrane separations.

The experimental relevance of this interaction remains unclear. To identify unambiguously the origin of intermembrane repulsion, it is crucial to carry out studies in uncharged systems. To date, studies[1] of neutral lipids have been limited to systems which exhibit a narrow range of intermembrane separations between $\sim$1.0 and 2.0 nm, where the long-range van der Waals and steric interactions are both expected to fall off as $1/d^2$. Moreover, these studies have been associated with lipid systems in which the membrane curvature elasticity[6] $k_c > 20 k_B T$, in which case van der Waals interactions are significantly larger. Thus, although the concept of this novel fluctuation-induced steric interaction has stimulated a large body of theoretical[7] and experimental[1,5] work, its significance in biological membranes remains largely controversial.

To elucidate the relevance of this interaction in multilayer systems, we report in this paper on a synchrotron diffuse x-ray scattering study in the lamellar L_α phase of the quaternary mixture of sodium dodecyl sulfate (SDS, the surfactant), pentanol (cosurfactant), water, and dodecane as a function of dodecane dilution. Figure 1 shows a cut of the phase diagram mapped out by Roux and Bellocq[8] represented on a standard triangular phase diagram in the plane with a constant water/SDS weight ratio equal to 1.55. This cut contains five one-phase regions: the microemulsion phases $\mu\varepsilon_1$ and $\mu\varepsilon_2$ and the liquid crystalline hexagonal (E), rectangular (R), and lamellar (L_α) phases.

The L_α phase consists of water layers (inverted membrane) embedded in oil, shown schematically in Fig. 1 with the fluid surfactant at the interface. This affords distinct advantages for studies of intermembrane interactions. First, the water layers are charge neutral so that there are no intermembrane electrostatic interactions. Second, and very significantly for this plane of the phase diagram, we are able to dilute over an unusually large oil range between 0 and 80 wt.%, which corresponds to intermembrane separations between $\sim$2.0 and larger than

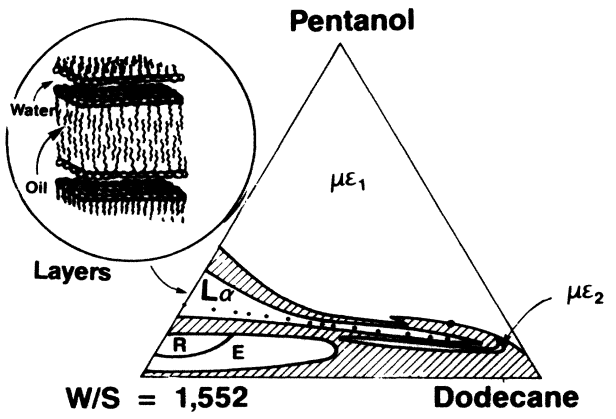

FIG. 1. A cut of the phase diagram of the quaternary mixture of SDS, pentanol, water, and dodecane shown in the plane with a constant water/SDS weight ratio = 1.55 (Ref. 8). The dots in the lamellar phase labeled L_α correspond to the mixtures studied.

20.0 nm. Third, previous work[9] on the curvature elasticity in similar microemulsion L_α phases had indicated unusually small values of $k_c \sim k_B T$. These unique properties of the microemulsion L_α phases[10] thus allow for a comprehensive study of the long-range van der Waals and steric interactions.

Landau and Peierls[5] first demonstrated that the mean square layer displacements of a system of stacked fluid layers diverge logarithmically, $\langle u^2 \rangle \sim \ln(L/a)$, with sample size L, destroying conventional long-range order (a is of order of the intermolecular distance). For the x-ray structure factor, the consequences are dramatic. Caillé[11] has shown that for a smectic-A liquid-crystal phase, which has the identical elastic free energy [Eq. (1)] as that for the L_α phase, conventional δ-function Bragg peaks at $(0,0,q_m = mq_0 = m2\pi/d)$ (harmonic order $m = 1,2,\ldots$) are replaced by singularities with asymptotic power-law behavior $S(0,0,q_z) \sim |q_z - q_m|^{-2+\eta_m}$ and $S(q_\perp,0,q_m) \sim q_\perp^{-4+2\eta_m}$. Here, $\eta_m = m^2 q_0^2 k_B T/8\pi \times (BK)^{1/2}$ and q_z and $q_\perp$ are components of the wave vector normal and parallel to the layers. This power-law behavior has been confirmed[12] for the first harmonic $q_z = q_0$ in the smectic-A phase of liquid crystals.

Here we find that the L_α phase of this SDS system corresponds to a Landau-Peierls system with characteristic power-law behavior for the first and second harmonics of the structure factor with η_m scaling as m^2. Most significantly we find that for intermembrane distance 3.8 nm $\leq d \leq$ 16.3 nm, η_1 is accurately described by $\eta_1(d) = 1.33(1 - \delta/d)^2$ predicted by the Helfrich theory[2] (δ is the membrane thickness). This then is a direct experimental confirmation of the Helfrich steric interaction mechanism and its dominant behavior in appropriate model multimembrane systems. Additionally, our measurements confirm that the membrane curvature elasticity $k_c \sim k_B T$.

We carried out detailed studies for ten distinct mixtures: $x = 0$, 0.07, 0.13, 0.18, 0.23, 0.29, 0.35, 0.47, 0.54, and 0.62 (labeled by closed circles in Fig. 1). Here, x is the percentage of dodecane by weight of the mixtures. For $x = 0$, 0.07, and 0.13, the first and second harmonics of the structure factor were studied with the second harmonic not visible for dilutions x larger than 0.13. The experiments were carried out at the Stanford Synchrotron Radiation Laboratory on beam line VI-2 and at the National Synchrotron Light Source on the Exxon beam line X-10A. The monochromator and analyzer consisted of a double-bounce Si(111) and a triple-bounce Si(111) channel-cut crystal set at 8 keV in the nondispersive configuration, which yields a very sharp in-plane Gaussian resolution function with very weak tail scattering with half width at half maximum (HWHM) 8×10^{-5} Å^{-1}. A sharp Gaussian out-of-plane resolution function (HWHM = 10^{-3} Å^{-1}) was achieved by use of extremely narrow slits. The mixtures were contained in sealed quartz capillaries with diameters of 1 and 2 mm, which yielded randomly oriented lamellar domains.

We show in Fig. 2 typical scattering profiles for longitudinal scans through the first harmonic for x between 0 and 0.54 in the L_α phase, where the total layer spacing $d = 2\pi/q_0$ increases from 3.82 to 11.5 nm. In the mixtures studied, the dilution corresponds to a path where water layers with approximately constant thickness d_w

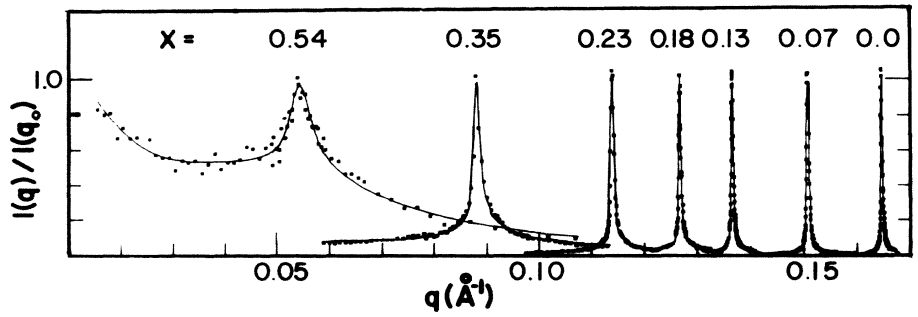

FIG. 2. Longitudinal profiles of the first harmonic of seven different mixtures along the dodecane dilution path. The percentage dodecane by weight of the mixtures (x) is indicated above each profile. All peak intensities are normalized to unity. The solid lines are fits by the Caillé power-law line shape [Eq. (2)].

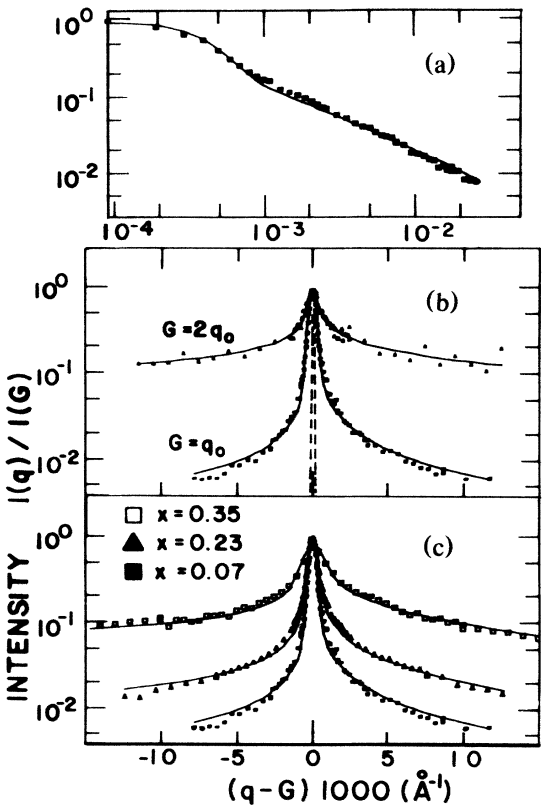

FIG. 3. (a) Profile of the first harmonic ($G=q_0$) for the mixture $x=0.23$ on a log-log scale which shows finite size rounding at small $q-G$ followed by power-law behavior at larger $q-G$. (b) Profile of the first and second harmonics for the mixture $x=0.07$ on a logarithmic intensity scale. (c) Profile of the first harmonic ($G=q_0$) for three mixtures on a logarithmic intensity scale. All peak intensities are normalized to unity. The solid lines are fits by the Caillé power-law line shape [Eq. (2)].

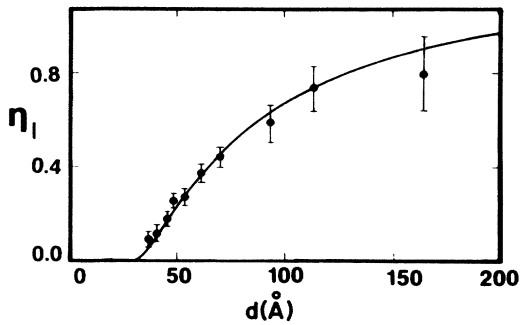

FIG. 4. Power-law exponent η_1 as a function of the intermembrane distance for mixtures along the dilution path. The solid line is the prediction of the model of Helfrich of entropically driven steric interactions.

~ 18 Å are pushed apart with d_0/d_w varying from ~ 1 to ~ 7. ($d_0=d-d_w$ is the oil thickness between water layers.) A striking feature of the profiles in Fig. 2 is the tail scattering which becomes dramatically more pronounced as d increases. This effect is further elucidated in Fig. 3(c), where we plot on a logarithmic intensity scale versus $q-q_0$ the scattering for three mixtures, $x=0.07$, 0.23, and 0.35. The significant difference in the profiles over the entire dilution range is now immediately clear. It is qualitatively clear that $\eta_1(d)$, which characterizes the asymptotic scattering profile and which is a measure of the ratio of the tail to peak intensity scattering, is increasing as d increases.

To analyze the profiles quantitatively, we begin with the Caillé[11] calculation. For a single crystal of infinite domain size in the L_α phase, the width of the measured profile at $q=q_0$ is primarily determined by the longitudinal resolution. Our very high-resolution setup can resolve length scales of 1.5 μm. The longitudinal resolution is shown dashed in Fig. 3(b). The widths of the profiles are normally 2 to 3 times larger than resolution. We find that for different preparations of the same mixture, the widths of the profiles may differ by as much as 50%. Thus, we attribute the broadening primarily to an extrinsic effect of finite lamellar domain sizes (associated with defects). The typical domain sizes are unusually large, between ~ 2500 and ~ 12500 Å, which allowed for meaningful analysis of the profiles.

We incorporate the finite-size effect in our analysis in a way analogous to that of Dutta and Sinha.[13] This modifies the structure factor $S(\mathbf{q})$ for an infinite single-crystal domain in a straightforward manner

$$S_{\text{F.S.}}(\mathbf{q}) \sim \int d^3R\, S(\mathbf{R}) e^{-R^2\pi/L^2} e^{i(\mathbf{q}-\mathbf{G})\cdot\mathbf{R}},$$

where L^3 is the domain volume and $\mathbf{G}=mq_0\hat{z}$. The correlation function $S(\mathbf{R})=S(z,\rho)\sim(1/\rho)^{2\eta}\exp\{-\eta \times[2\gamma+E_1(\rho^2/4\lambda z)]\}$ was calculated by Caillé.[11] Here $R^2=z^2+\rho^2$, γ is Euler's constant, $E_1(x)$ is the exponential integral function, and $\lambda=(K/B)^{1/2}$. Finally, because our samples consist of randomly oriented domains, we perform an exact powder average over all solid angles in reciprocal space:

$$\langle S(\mathbf{q})_{\text{F.S.}}\rangle \equiv S(q) \sim \int_{-\infty}^{\infty} dz \int_0^{\infty} d\rho\, S(z,\rho) e^{-R^2\pi/L^2} [(\sin qR)/qR] e^{-iGz}. \quad (2)$$

The analysis consists of least-squares fits of Eq. (2) convoluted with the resolution function to the observed profiles. We plot in Fig. 3(a) on a log-log scale the intensity versus $q-q_0$ for $x=0.23$, where the solid line is a result of the fit yielding $\eta_1=0.25$ and $L=8640$ Å. Two features in the scattering profile and the theoretical cross section are immediately apparent. While at large $q-q_0 \gtrsim 2\pi/L$ the scattering exhibits power-law behavior $S(q) \sim |q-q_0|^{-P}$ with $P\sim 1-\eta$ at $q\simeq q_0$, the finite-size effects round off the observed profile with characteristic width $\sim 1/L$. (This effective power-law exponent P is due to the powder averaging.)

A further, more subtle aspect of the data is evident in Fig. 3(c), where the profiles around $q=q_0$ are slightly asymmetric with the high-q scattering more intense than the low q. The parameter $\lambda \equiv (K/B)^{1/2}$, which enters the real-space correlation function $S(\mathbf{R})$, is a measure of the degree of anisotropy present in $S_{\text{F.S.}}(q_z, q_\perp)$.[11] The powder average of this anisotropic scattering cross section results in the observed asymmetric profile. For $\lambda > 2\pi/q_0$ the asymmetry is negligible and $S(q)$ is not very sensitive to the precise value of λ.

To summarize the essential points in the fits, the four parameters q_0, η, L, and λ are given respectively by the peak position, the power-law behavior away from the Bragg point, the central-peak width, and the asymmetry in the profile around the Bragg point. As is evident from the typical results of fits shown in Figs. 2 and 3, where η_1 varies by more than a factor of 7 (Fig. 4), the appropriately modified finite-size and powder-averaged Caillé cross section gives a quantitatively satisfactory description of the scattering. In contrast to the smectic-A system[12] where only the first harmonic was evident, we are able to confirm the scaling of η_m with m^2. We show in Fig. 3(b) the profiles and fits for the first and second harmonics for $x=0.07$ on a normalized logarithmic intensity scale. We find $\eta_1(q_0)=0.14\pm0.02$, $\lambda=8.59\pm1$, $L=(10027\pm1000)$ Å for the first harmonic and $\eta_2(2q_0)=0.575\pm0.02$, $\lambda=8.13\pm2$, $L=(9115\pm1500)$ Å for the second harmonic. We also confirmed the scaling of η with m^2 for the mixtures $x=0$ and $x=0.13$.

For the last three dilutions ($x=0.47$, 0.54, and 0.62) as seen in Fig. 2 for $x=0.54$, in addition to the first harmonic, the data exhibited small-angle x-ray scattering (SAXS). For $0.8>x>0.62$ the SAXS dominates, although the existence of focal conics observed in optical microscopy indicates a lamellar structure. Although we do not understand the origin of the SAXS (possibly due to defects), we are able to fit the SAXS for samples in the range $0.8>x>0.62$ with a simple model[14] of polydisperse spheres with the same radius ($\sim$100 Å) but varying intensities. Accordingly, the fit to the profile for $x=0.47$, 0.54, and 0.62 involves one more adjustable parameter which is the SAXS intensity.

We find that λ increases smoothly between 5 and 25 Å for $0<x<0.62$. The elastic constants B and $k_c(=Kd)$ are derived from η and λ. The magnitude of B ranges from typical smectic-A values[12] (6×10^7 erg/cm^3) to more than 2 orders of magnitude less for large dilutions. In contrast k_c, which is the membrane-bending modulus, varies slowly. Very significantly, we find that $k_c\sim(0.5$ to $2.0)k_BT$ is about an order of magnitude smaller than that measured in other model membrane systems. Therefore, since the Helfrich mechanism scales as k_c^{-1}, we expect this interaction U_s/A, which ranges between $0.12k_BT/d^2$ and $0.46k_BT/d^2$, to dominate the van der Waals interaction $U_{\text{vdW}}/A\sim-0.03k_BT/d^2$.

We plot in Fig. 4 $\eta_1(d)$ resulting from fits to the profile at the first harmonic as a function of d. The solid line, which agrees well with the experimental data, is a plot of the predicted value for $\eta_1(d)=1.33(1-\delta/d)^2$ derived from the Helfrich theory. Here, we have taken the effective water thickness $\delta=29$ Å slightly larger than d_w because of the known excluded volume effects[8] of the surfactant tails in the oil. *This then provides compelling evidence that in this SDS multimembrane system the intermembrane interactions are dominated by the Helfrich mechanism of entropically driven steric interactions.*

We gratefully acknowledge useful discussions with S. Alexander, R. J. Birgeneau, K. D'Amico, P. G. de Gennes, S. Leibler, S. Mochrie, D. E. Moncton, P. Pincus, J. Prost, and S. Safran. It is a pleasure to acknowledge assistance from the Exxon staff members at the Exxon beam line, especially R. Hewitt and M. Sansone. The National Synchrotron Light Source, Brookhaven National Laboratory, and the Stanford Synchrotron Radiation Laboratory are supported by the U. S. Department of Energy. A part of the research was supported by a joint Industry/University National Science Foundation Grant No. DMR-8307157.

[1]J. N. Israelachvili, *Intermolecular and Surface Forces* (Academic, Orlando, 1985); V. A. Parsegian, N. Fuller, R. P. Rand, Proc. Natl. Acad. Sci. **76**, 2750 (1979).

[2]W. Helfrich, Z. Naturforsch. **33a**, 305 (1978).

[3]S. G. J. Mochrie, A. R. Kortan, R. J. Birgeneau, and P. M. Horn, Z. Phys. B **62**, 79 (1985).

[4]P. G. de Gennes, *The Physics of Liquid Crystals* (Clarendon, Oxford, 1974).

[5]L. D. Landau, in *Collected Papers of L. S. Landau,* edited by D. Ter Haar (Gordon and Breach, New York, 1965), p. 209; R. E. Peierls, Helv. Phys. Acta. **7**, Suppl., 81 (1934).

[6]M. B. Schneider, J. T. Jenkins, and W. W. Webb, J. Phys. (Paris) **45**, 1457 (1984).

[7]R. Lipowsky and S. Leibler, Phys. Rev. Lett. **56**, 2561 (1986), and references therein.

[8]D. Roux and A. M. Bellocq, *Physics of Amphiphiles,* edited by V. DeGiorgio and M. Corti (North-Holland, Amsterdam, 1985).

[9]J. M. diMeglio, M. Dvolaitsky, and C. Taupin, J. Phys. Chem. **89**, 871 (1985).

[10]F. C. Larché, J. Appell, G. Porte, P. Bassereau, and J. Marignan, Phys. Rev. Lett. **56**, 1700 (1986).

[11]A. Caillé, C. R. Acad. Sci. Ser. B **274**, 891 (1972).

[12]J. Als-Nielsen, J. D. Litster, R. J. Birgeneau, M. Kaplan, C. R. Safinya, A. Lindegaard-Andersen, and S. Mathiesen, Phys. Rev. B **22**, 312 (1980).

[13]P. Dutta and S. K. Sinha, Phys. Rev. Lett. **47**, 50 (1981).

[14]A. Guinier, *X-Ray Diffraction* (W. H. Freeman, New York, 1963).